

■ Isotopic variation in Semail Ophiolite lower crust reveals crustal-level melt aggregation

M.N. Jansen, C.J. Lissenberg, M. Klaver, S.J. de Graaff, J.M. Koornneef, R.J. Smeets, C.J. MacLeod, G.R. Davies

■ Supplementary Information

The Supplementary Information includes:

- Extended Analytical Techniques and Data Treatment
- Tables S-1 to S-3
- Figures S-1 and S-2
- Supplementary Data Table (Table S-4; Excel download)
- Supplementary Information References

Extended Analytical Techniques and Data Treatment

1. Mineral major and trace element analysis

Mineral major and trace element data of OC and OG coded samples are published in MacLeod and Yaouancq (2000) and Thomas (2003). Carbon-coated polished thick-sections (200 μm) were produced from the OM samples lacking mineral data. Major element compositions were determined at the Vrije Universiteit Amsterdam with a JEOL JXA 8800M electron microprobe (EMP) at an acceleration voltage of 15 kV and a beam current of 25 nA (clinopyroxene) and 15–20 nA (plagioclase). Pyroxenes were analysed with a focused beam whereas plagioclase was analysed with a spot size of 10 μm . Analyses were matrix-corrected using the ZAF method and calibrated against natural and synthetic mineral standards. Two plagioclase and clinopyroxene grains were analysed in each sample and within each grain five spots were analysed in the core and five near the rim (distance from rim ≥ 10 μm). Mineral compositions were checked for mineral stoichiometry by normalising results to 8 atoms per formula units (apfu) O for plagioclase and 6 apfu O for pyroxene. Analyses were excluded if the sum of cations was <99.5 % or >100.5 % (for clinopyroxene) and <99.0 % or >101.0 % (for plagioclase) or if the sum of oxides was <98.5 % or >101.5 %.

Trace element concentrations in clinopyroxene and plagioclase (for the OM samples) were determined in situ by laser-ablation inductively-coupled plasma-mass spectrometry (LA-ICPMS) at the Institute of Mineralogy, Westfälische Wilhelms Universität Münster, Germany. The ablation system consisted of a 193 nm excimer laser (Analyte G2, Photon Machines) coupled to an Element 2 (Thermo Fisher Scientific) single collector mass spectrometer. The laser was operated at an energy density of ~ 4 J/cm² and a spot size between 65 and 85 μm . A NIST 612 glass reference material was used as external calibration standard while glasses of BCR2-G and BIR1-G reference materials were used as secondary standards. The CaO concentrations determined by EMP were used as internal standard element (⁴³Ca) for quantification (average CaO concentrations in the sample were used as internal standard element where it was not possible to analyse the same grains analysed by EMP). Overall measurement time for single spot analysis was 60 s, with 20 s background and 40 s on peak signal. Raw data were processed using GLITTER software (Griffin *et al.*, 2008). Two clinopyroxene



and two plagioclase crystals were analysed for each sample, where possible the same grains that were analysed with EMP. For each grain, two spots were placed in the core and two were placed near the rim ($\geq 10 \mu\text{m}$). Glass reference materials BCR2-G and BIR1-G were used to monitor precision and accuracy ($n = 10$ and 8 , respectively), in the absence of appropriate clinopyroxene and plagioclase trace element standards. Reproducibility of key trace elements was better than 10 % (2 RSD), but reproducibility of trace element ratios (e.g., Sm/Nd) was better than 6 % (2 RSD) (see Table S-1). It should be noted that clinopyroxene and plagioclase from this study have trace elements compositions that are not entirely comparable to the BCR2-G and BIR1-G reference materials (basalts). However, for the purposes of this study, the Nd and Sm concentrations in clinopyroxene are of primary interest (for the age corrections, see also Section 5). These concentrations are of the same order of magnitude as in BIR1-G reference material, making it a suitable external standard.

Table S-1 Reproducibility of key trace elements and ratios (2 RSD).

	Number of analyses	Cr	Rb	Sr	La	Ce	Pr	Nd	Sm	Eu	Gd	Tb	Dy
BCR2-G	10	4.5%	2.8%	5.3%	1.4%	2.1%	2.1%	2.0%	2.9%	4.0%	2.0%	7.3%	6.2%
BIR1-G	8	3.4%	3.4%	17.2%	1.2%	4.5%	4.3%	4.6%	6.8%	9.9%	3.8%	10.2%	7.9%
	Number of analyses	Ho	Er	Tm	Yb	Lu	Hf	Pb	Th	U	Sm/Nd	Rb/Sr	U/Pb
BCR2-G	10	6.3%	6.8%	6.8%	5.7%	7.2%	3.7%	17.9%	5.4%	3.0%	5.4%	4.7%	16.0%
BIR1-G	8	9.2%	7.5%	8.9%	7.2%	7.8%	8.7%	16.2%	14.9%	22.8%	5.3%	16.7%	21.0%

2. Sample processing and micro-sampling

Selected hand samples were cut with a diamond blade saw into rock slabs of 1-2 cm thick, perpendicular to the foliation and parallel to the lineation. The surfaces of these slabs were polished and within each sample the largest, least altered and inclusion-free plagioclase and clinopyroxene crystals were selected using a binocular microscope (Fig. S-1). Energy-dispersive elemental maps of these crystals were made at Cardiff University with a Zeiss Sigma HD Analytical SEM equipped with dual 150 mm² EDS detectors to reveal any cryptic major element zoning (Ca, Mg and Fe for clinopyroxene; Ca and Na for plagioclase).

Individual crystals and crystal domains (cores, rims) were micro-sampled at the Vrije Universiteit using a Merchantek MicroMill that was operated in a laminar flowhood and Horico diamond coated drill bits with a diameter of $\sim 500 \mu\text{m}$. Similar micro-sampling techniques have been applied successfully in previous studies for Sm-Nd isotope analysis in single garnets (Pollington and Baxter, 2011) and for Rb-Sr isotope analysis in single plagioclase crystals (Charlier *et al.*, 2006). Before use, drill bits were cleaned by submerging them in 0.165 M HCl for 1 s and washing them in a Milli-Q water (Millipore B.V.) ultrasonic bath for 15 minutes. For micro-sampling single crystals, care was taken to avoid the immediate area near grain boundaries, where the effects of diffusion, melt-rock reactions and low temperature alteration are expected to be largest. Before drilling, the carbon coat was removed and the surfaces of the rock slabs were cleaned stepwise with Milli-Q water (60 s), ethanol (60 s), and 1 M acetic acid (30 s). Subsequently slabs were placed in a Milli-Q water ultrasonic bath for 10 minutes. See Table S-2 for blank levels determined for the micro-sampling procedure by placing a drop of Milli-Q water on a rock slab for 1-60 minutes. When drilling multiple crystals from the same rock slab, the slab was cleaned with Milli-Q water and ethanol before drilling the next crystal. The rock slabs were mounted onto the micromill stage and secured with wax. The stage offset calibration procedure requires a small hole to be drilled in the rock slab at a random location. To remove any (minor) contamination resulting from this procedure, the drill bit is submerged in a Milli-Q water drop for thirty seconds while it was rotating. After stage offset and drill-bit position calibrations were completed, a line path was drawn on the selected crystal to be traced by the drill. Paths were drawn to maximise the surface area drilled while avoiding inclusions and maintaining a distance of $\sim 0.1 \text{ mm}$ from the grain boundaries. Large grains ($> 1\text{-}2 \text{ mm}$) that displayed core-to-rim major element zoning, core and rim samples were drilled sequentially. During micro-sampling, the drilled material was brought into suspension by placing a drop of Milli-Q water at the drilling spot. The Milli-Q water containing the drilled sample was pipetted into a pre-cleaned 7 ml PFA beaker and new drops were placed near the drill at regular time intervals during drilling. Drilling speed was set to 65 % and scan- and drill plunge speeds were kept low (20-30 $\mu\text{m/s}$) to avoid interlock failures due to the hardness of the crystals. The duration of micro-sampling, measured from the moment of placing of the Milli-Q water drop to the pipetting of the last material, varied between 10 to 70 minutes per grain for most samples. After drilling was completed, the optically determined dimensions and shape of the hole were used to estimate the volume sampled.



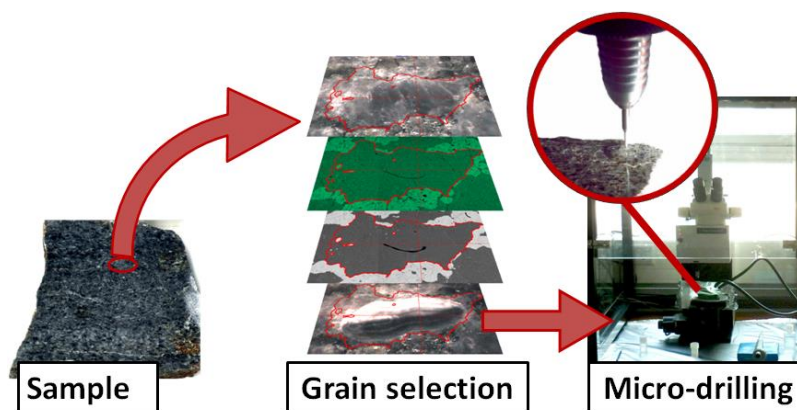


Figure S-1 Schematic workflow of the micro-sampling procedure: samples cut into rock slabs were examined under the microscope and the best-preserved grains were selected. Major element maps and backscattered electron images of the selected grains were used to identify zoning and/or inclusions. On basis of this information the crystal was sampled along a drilling pattern using a Merchantek MicroMill.

3. Sample digestion and ion-exchange chromatography

Samples recovered from the micromill were dried down and subsequently digested in PFA beakers in 1 ml of a 1:4 mixture of concentrated HNO_3 and HF on a hotplate at 140 °C for ≥ 48 hours. An aliquot of a ^{149}Sm - ^{150}Nd mixed-spike was added to plagioclase samples prior to digestion for isotope dilution analysis of Nd and Sm concentrations. All reagents used in this study were double sub-boiling distilled to achieve low blank levels. After digestion, samples were dissolved in 0.5 ml 2.0 M HNO_3 . Resins for ion-exchange chromatography were obtained from Eichrom Technologies, Inc. The light rare-earth elements (LREE) were separated from the matrix using 150 μl TRU resin columns by eluting the matrix with 3.75 ml 2.0 M HNO_3 (elution volume is including the 0.5 ml sample load) and eluting the LREE fraction with 1.5 ml Milli-Q water. For plagioclase samples, the matrix was collected and subsequently dried down, re-dissolved in 0.5 ml 3.0 M HNO_3 , and loaded onto 75 μl Sr resin columns. Sr was eluted with 1.0 ml Milli-Q water following the elution of the matrix with 2.25 ml 3.0 M HNO_3 . Sr isotopes in clinopyroxene are not expected to reflect the magmatic source due to high diffusion rates and sensitivity to hydrothermal alteration (Sneeringer *et al.*, 1984; Kempton and Hunter, 1997) and were therefore not considered herein. The REE fraction was dried down, re-dissolved in 0.5 ml 0.165 M HCl and loaded onto 0.75 ml Ln resin columns. After elution of the La, Ce and the bulk of Pr (9.5 ml 0.165 M HCl), Nd was eluted with 4.0 ml 0.3 M HCl, followed by Sm elution for ID samples using 5.0 ml of 0.5 M HCl. Collected Sr, Nd and Sm fractions were dried down and treated with concentrated HNO_3 prior to TIMS analysis. Total procedural blanks are listed in Table S-2 and are typically $<1\%$ of the sample size for Nd and Sm and $<1\%$ for Sr, and thus considered to be negligible.

Table S-2 Blanks determined by isotope dilution for the micro-sampling procedure, the total cleanroom procedural blank (digestion and ion-exchange chromatography) and typical loading blanks. These values are consistent with other studies from the same laboratory (*e.g.*, Klaver, 2016). n.d. – not determined. b.d.l. – below detection limit.

		Nd (pg)	Sr (pg)	Sm (pg)
Microsampling procedure	1 min. of drilling	0.07	61	n.d.
	60 min. of drilling	b.d.l.	59	n.d.
Cleanroom procedure	Plagioclase series	0.96	30.2	0.29
	Clinopyroxene series	0.59-5.81	17.0-57.7	n.d.
Loading blank		<0.01	3	n.d.

4. TIMS analyses

Isotopic analyses were performed using a Thermo Scientific Triton *Plus* thermal ionisation mass spectrometer (TIMS) at the Vrije Universiteit Amsterdam using single (Sr) and double (Nd and Sm) annealed Re filaments. Whereas sufficient Sr was available to follow regular analytical protocols (*e.g.*, Font *et al.*, 2012), low amounts of Nd (200-600 pg) and Sm (50-250 pg) in the plagioclase samples required the use of $10^{13} \Omega$ resistors fitted in the Faraday cup amplifier feedback loop (hereafter referred to as " $10^{13} \Omega$ ").



amplifiers"; Koornneef *et al.*, 2014; Klaver *et al.*, 2016).

Strontium samples were loaded together with 2 μl of a TaCl_5 activator (concentration = 10 $\mu\text{g Ta}/\mu\text{l}$) to enhance ionisation. Measurements were carried out in static multi-collection mode using default 10^{11} Ω amplifiers at ^{88}Sr ion beam currents of $\sim 4.5 \times 10^{-12}$ A (equivalent to a signal intensity of 4.5 V) for 200 cycles of 8.4 s integration time with a 30 s baseline measurement every 20 cycles. Instrumental mass fractionation was corrected for by normalising to $^{88}\text{Sr}/^{86}\text{Sr} = 8.375209$ using the exponential law (Thirlwall, 1991) and data were subjected to an online 2 SD outlier test. Isobaric interference of Rb was monitored at mass 85 but was found to be negligible and hence no correction was required for interference of ^{87}Rb on ^{87}Sr . Repeated analyses of NIST SRM 987 yielded $^{87}\text{Sr}/^{86}\text{Sr} = 0.710257 \pm 34$ (2 SD; $n = 11$) over the course of this study. All data are reported relative to $^{87}\text{Sr}/^{86}\text{Sr} = 0.710245$ for SRM 987. Due to low Rb concentrations (< 0.05 ppm; Supplementary Data Table) in plagioclase, ingrowth of ^{87}Sr after crystallisation was assumed to be negligible and hence no age correction was applied.

Neodymium and samarium samples were loaded on double filaments together with 1 μl 1% H_3PO_4 . Clinopyroxene samples contained sufficient Nd (3–6 ng) for analysis with default 10^{11} Ω amplifiers whereas the low amounts of Nd and Sm in plagioclase samples necessitated the use of 10^{13} Ω amplifiers (Table S-3) to improve the signal-to-noise ratio by a theoretical factor of 10. In practice, however, an improvement of a factor ~ 2 –3 in external precision (reproducibility) can be achieved with the use of 10^{13} Ω amplifiers (Koornneef *et al.*, 2014; Klaver *et al.*, 2016). A similar measurement strategy is followed for all Nd and Sm analyses, regardless of amplifiers used. A 660 s baseline measurement was conducted during filament warm-up to allow continuous data acquisition afterwards. Data acquisition was started at low signal intensities, directly after beam optimisation and peak centring, and samples were run to exhaustion. The signal was monitored continuously during measurement and filament currents were adjusted to keep the ion beam as stable as possible. Measurement durations varied between 16 and > 200 cycles of 8.4 s integration time, with an average of 115 cycles for Nd in clinopyroxene, 270 cycles for Nd in plagioclase samples and 150 cycles for Sm in plagioclase. The use of 10^{13} Ω amplifiers necessitated an external gain calibration as online calibration using an internal reference current (0.333333 pA) was not possible. The La Jolla Nd standard was used to determine gain factors for these amplifiers following Trinquier (2014). The 10^{13} Ω amplifiers were assigned to different cups through the Triton amplifier relay board and ^{144}Nd and ^{146}Nd (the most abundant measured Nd isotopes) were measured on default, gain-corrected 10^{11} Ω amplifiers (Table S-3). This allowed correction for instrumental mass fractionation to $^{146}\text{Nd}/^{144}\text{Nd} = 0.721903$. Any residual offset between measured $^{143}\text{Nd}/^{144}\text{Nd}$, $^{145}\text{Nd}/^{144}\text{Nd}$, $^{148}\text{Nd}/^{144}\text{Nd}$ and $^{150}\text{Nd}/^{144}\text{Nd}$ and the long-term average was then ascribed to variations in amplifier gain. Gain factors were calculated in this way on a daily basis and entered in the amplifier system table of the Triton software such that gain corrections were performed automatically online. All measurements were then corrected offline for a 3-month average of the gain factors (September – November 2015, during which analyses in this study were performed; $n = 27$). The robustness of gain factors calculated in such a way was shown by Klaver *et al.* (2016) and any residual scatter introduced by this method is accounted for by incorporating the reproducibility of secondary standards measured at the same conditions in the quoted measurement uncertainties (see below).

Data reduction was performed offline to allow deconvolution of the spike contribution in the isotope-dilution runs. Clinopyroxene data were filtered to include only ratios measured at ^{143}Nd currents of ≥ 1.0 pA (equivalent to 100 mV signal intensity on a default 10^{11} Ω amplifier) where possible, but for two samples data acquired at lower currents were included (sample 95OG16-cpx-core at ≥ 0.3 pA; sample 95OC41-cpx at ≥ 0.5 pA; equivalent to 30 and 50 mV on a default 10^{11} Ω amplifier, respectively). For clinopyroxene samples, no further outliers were removed unless they were conspicuously related to signal instability. Plagioclase data were filtered to include only ratios measured at ^{143}Nd currents of ≥ 0.05 pA (equivalent to 5 mV signal intensity on a default 10^{11} Ω amplifier) and subsequently subjected to a 2 SD outlier test. Isobaric interference of Sm on ^{144}Nd and ^{150}Nd was monitored at mass ^{147}Sm . Two samples (14OM4-plg-id3 and 14OM5-plg-id) showed minor Sm interference ($^{147}\text{Sm}/^{144}\text{Nd} < 0.0005$) during the Nd measurement, which was corrected by calculating the Sm composition (mass 144 and 150) of the spike-sample mix and subtracting that from the raw ^{144}Nd and ^{150}Nd data, respectively. Only Sm isotopes free from Nd interference were used in the data reduction and Gd was quantitatively removed during chemical separation, hence no interference correction was required (Table S-3). The raw data were corrected for instrumental mass fractionation and spike contribution following the iterative approach described by Stracke *et al.* (2014) and by normalising to $^{146}\text{Nd}/^{144}\text{Nd} = 0.721903$ and $^{147}\text{Sm}/^{152}\text{Sm} = 0.56081$ (Carlson *et al.*, 2007) on a cycle-by-cycle basis. Resultant average $^{150}\text{Nd}/^{144}\text{Nd}$ and $^{149}\text{Sm}/^{152}\text{Sm}$ were used to calculate Nd and Sm concentrations following standard isotope dilution equations. This spike-stripping approach has been demonstrated to yield accurate and precise $^{143}\text{Nd}/^{144}\text{Nd}$ data even at high spike-sample ratios (Stracke *et al.*, 2014). Nevertheless, samples were underspiked by a factor 10–20 to mitigate any potential effect of spike contribution on the isotope composition, which resulted in only a marginal increase in error magnification for Sm and Nd concentrations. The uncertainty on Sm/Nd as determined by isotope dilution is estimated from the long-term reproducibility of USGS reference materials BHVO-2 and BCR-2 (measured on regular sample sizes) to be better than 0.5 %.



Table S-3 Cup configuration and use of detectors for Nd and Sm measurements. Interfering elements are shown in italics. Notes: *isotope used for instrumental mass fractionation correction to determine gain factors for the 10¹³ Ω amplifiers; †isotope used for isotope dilution data reduction, note that these isotopes suffer no Nd interference and are hence not influenced by the presence of small amounts of Nd.

Faraday cup	L3	L2	L1	axial	H1	H2	H3	H4
Nd	¹⁴³ Nd	¹⁴⁴ Nd	¹⁴⁵ Nd	¹⁴⁶ Nd	¹⁴⁷ Sm	¹⁴⁸ Nd	-	¹⁵⁰ Nd
<i>Interference (abundance %)</i>		¹⁴⁴ Sm (3.1)				¹⁴⁸ Sm (11.2)		¹⁵⁰ Sm (7.4)
Clinopyroxene	10 ¹¹ Ω	10 ¹¹ Ω	10 ¹¹ Ω	10 ¹¹ Ω	10 ¹¹ Ω	10 ¹¹ Ω	-	10 ¹¹ Ω
Plagioclase	10¹³ Ω	10¹³ Ω	10 ¹¹ Ω	10¹³ Ω	10 ¹¹ Ω	10 ¹¹ Ω	-	10¹³ Ω
Gain calibration	10¹³ Ω	10¹¹ Ω*	10¹³ Ω	10¹¹ Ω*	10 ¹¹ Ω	10¹³ Ω	-	10¹³ Ω
Sm	¹⁴⁶ Nd	¹⁴⁷ Sm†	¹⁴⁸ Sm	¹⁴⁹ Sm†	¹⁵⁰ Sm	¹⁵² Sm†	-	-
<i>Interference (abundance %)</i>			¹⁴⁸ Nd (5.7)		¹⁵⁰ Nd (5.6)	¹⁵² Gd (0.2)		
Plagioclase	10 ¹¹ Ω	10¹³ Ω	10¹³ Ω	10¹³ Ω	10 ¹¹ Ω	10¹³ Ω	-	-

5. Data quality and treatment of uncertainties

In the absence of obvious temporal drift in gain factors, the 3-month average gain factors were used to recalculate all raw data offline. Reproducibility of ¹⁴³Nd/¹⁴⁴Nd for standards measured with 10¹³ Ω amplifiers after gain calibration was 148 ppm (2 RSD) for artificial standard CIGO (mean = 0.511373 ± 0.000076; n = 23; various amounts ranging 0.3-250 ng Nd) and 161 ppm for BCR-2 reference material (mean = 0.512644 ± 0.000082; n = 11; 0.15-0.34 ng Nd) (Fig. S-2, Table S-4f). Repeated analyses of ¹⁴³Nd/¹⁴⁴Nd for standards measured with regular 10¹¹ Ω amplifiers were reproducible at 82 ppm for BCR-2 reference material (mean = 0.512630 ± 0.000042; n = 12; 1.9-2.6 ng Nd) and 73 ppm for BHVO-2 reference material (mean = 0.512972 ± 0.000038; n = 12; 1.6-2.1 ng Nd). Standards were measured at similar signal intensities and measurement durations as samples.

The reproducibility of ¹⁴³Nd/¹⁴⁴Nd of samples was determined through repeated analyses of BCR-2 reference material (Fig. S-2, Table S-4f). The BCR-2 aliquots were chosen to match the size of clinopyroxene samples (2.5 ng, n = 12) and plagioclase samples (0.15-0.35 ng, n = 11), respectively, and processed using the same procedures as the samples. The reproducibility of BCR-2 was then assessed using the mean square weighted deviation (MSWD), a statistic commonly used for determining the significance of isochrons (Eqs. S-1 and S-2; Wendt and Carl, 1991). A MSWD value of 1 implies that the data fit perfectly to a homogenous composition and that the amount of scatter is in agreement with predictions based on the analytical uncertainties. The MSWD of the two sets of BCR-2 aliquots was found to be greater than 1 (Fig. S-2, centre panels), indicating that the internal precision of the individual measurements cannot account for the full variation in ¹⁴³Nd/¹⁴⁴Nd. The excess variance, here named *x*², appears to be intrinsic to the measurement of small samples and is, amongst others, related to the fluctuation of the 10¹³ Ω amplifier gain values during an analytical session. The true reproducibility can therefore be expressed as the quadratic sum of the measurement uncertainty and the excess variance *x* (Eq. S-3).

$$Weighted\ Mean = \frac{\sum \frac{1}{\sigma_i^2} \times obs_i}{\sum \frac{1}{\sigma_i^2}} \tag{Eq. S-1}$$

$$MSWD = \frac{\sum \left(\frac{obs_i - weighted\ mean}{\sigma_i} \right)^2}{f} \tag{Eq. S-2}$$

$$Full\ error\ of\ measurement = \sqrt{standard\ error\ of\ measurement^2 + x^2} \tag{Eq. S-3}$$

where *obs_i* is the ¹⁴³Nd/¹⁴⁴Nd ratio of measurement *i*, *σ_i* is the uncertainty of measurement *i*, *f* is the degrees of freedom (in the case of this study *f* = *n* - 1), and *x*² is the excess variance.

Since the BCR-2 aliquots represent a homogeneous population, their MSWD value should equal 1 and based on this assumption the excess variance *x*² can be easily calculated in a process of iteration by solving Equations S-2 and S-3 until MSWD = 1. The resulting *x*² was found to be 0.000065 for plagioclase sample sizes and 0.000034 for clinopyroxene sample sizes (2 SD). Although the excess



variance is expected to be constant regardless of sample size, the gain calibration procedure for the $10^{13} \Omega$ amplifiers on the TIMS is known to introduce residual scatter in the measurements (Klaver, 2016) and probably affected the plagioclase analyses. Fully propagated uncertainties for Nd isotope measurements on samples were obtained with Equation S-3 using the measurement standard error and the corresponding excess variance.

Plagioclase $^{143}\text{Nd}/^{144}\text{Nd}$ ratios were age corrected (96 Ma) using the Sm/Nd ratios obtained from ID-TIMS and the corresponding uncertainties were propagated. For clinopyroxene samples the average Sm and Nd concentrations from LA-ICPMS spots on the thick-sections were used (*i.e.* from crystals coexisting in the same hand sample). Sm/Nd ratios in clinopyroxene ranged from 0.38 and 0.8 and the typical variability of Sm/Nd in one hand sample was between 0.05 and 0.2, which corresponds to a variability between 0.000019 and 0.000076 in the initial $^{143}\text{Nd}/^{144}\text{Nd}$. Most of the cited Sm/Nd variability, however, occurs within individual grains rather than between grains within a hand sample, thus justifying the average Sm/Nd ratio of coexisting grains as a reasonable estimate for the purpose of age corrections. The uncertainty on the Sm/Nd ratio (Table S-1) was propagated in the age correction calculations.

To quantify the variability in Nd isotopes in the plagioclase and clinopyroxene samples, the MSWD value was calculated using the fully propagated uncertainties, which was then compared to a critical MSWD value to evaluate the significance of the deviation from 1 (homogeneity). The critical value is based on the criteria Wendt and Carl (1991) give for rejecting the hypothesis that the set of measurements represent an isochron:

$$MSWD > 1 + 2\sqrt{\frac{2}{f}} \quad \text{Eq. S-4}$$

where f is the degrees of freedom ($n - 1$). This equation is derived from the variance of the theoretical MSWD frequency distribution and represents the upper limit of a 2σ confidence interval (Wendt and Carl, 1991). We note that the critical value (*i.e.* the right side of Eq. S-4) is dependent on the total number of analyses (n).



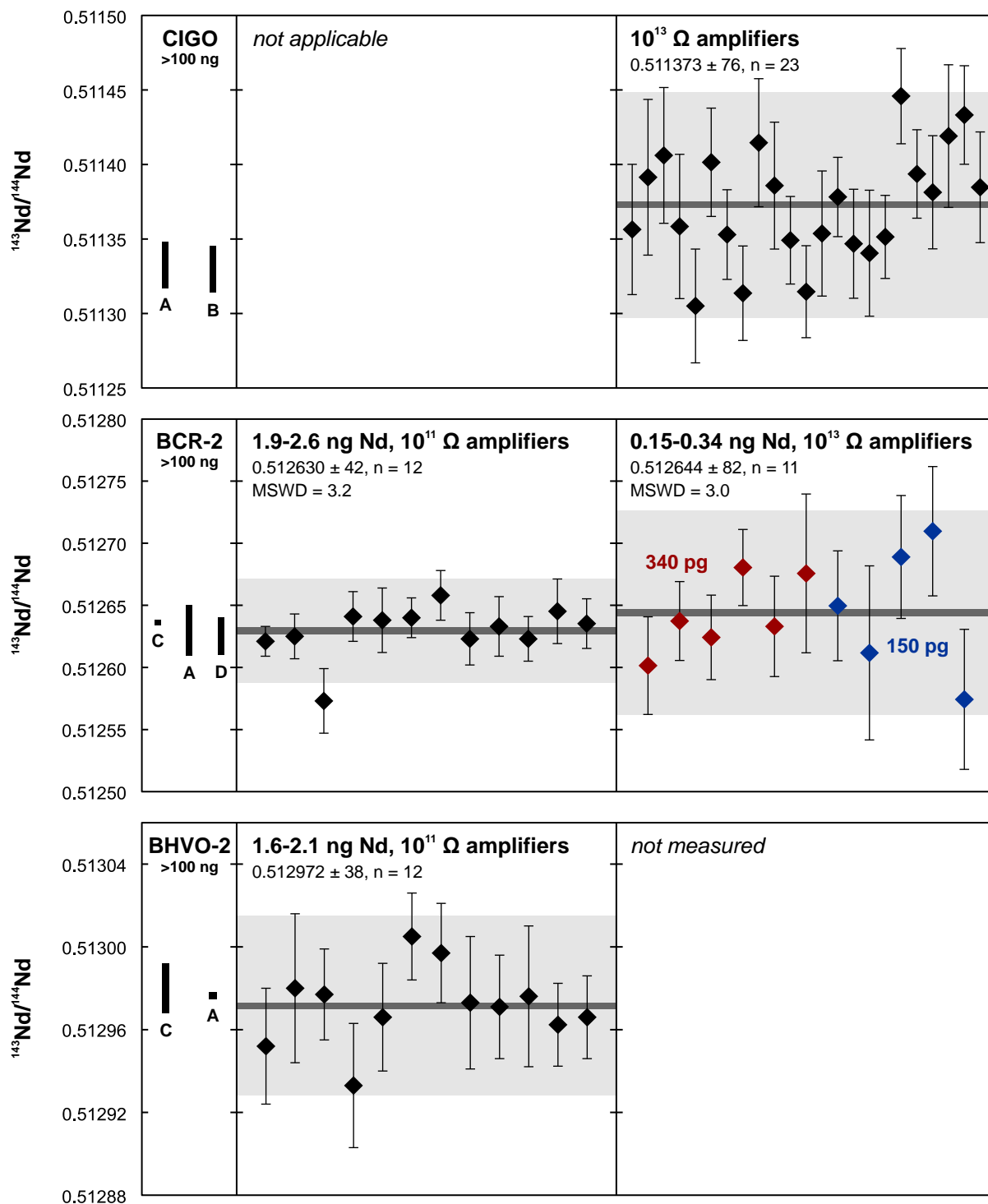


Figure S-2 Nd isotope data for reference materials measured over the course of this study. CIGO is the Vrije Universiteit in-house Nd standard made from Nd₂O₃ powder; the reference value is 0.511342, which relates to La Jolla = 0.511852 (Griselin *et al.*, 2001). Aliquots of USGS standards BHVO-2 and BCR-2 at the same size as samples (~2 ng Nd for clinopyroxene, ~0.3 ng Nd for plagioclase) were measured to assess the reproducibility of the method. These data points reflect aliquots of standard that were processed individually through the chemical separation process. The MSWD was calculated using internal precisions only and values greater than 1 indicate an (analytically related) excess variance, as discussed in the text. Notes: A – 2011-2015 average from Klaver (2016) (n = 39 for CIGO, n = 9 for BCR-2, n = 4 for BHVO-2); B – average of large (>200 ng) CIGO standards measured over the course of this study (0.511329 ± 0.000016, n = 29); C – preferred value from the GeoReM database (Jochum *et al.*, 2005); D – result for spike-stripped, ~200 ng Nd BCR-2 that was spiked for isotope dilution analysis. All error bars are 2 SE (internal precision). Grey field and bar indicate average and 2 SD. All quoted uncertainties are 2 SD.



Supplementary Data Table (Table S-4)

The Supplementary data table (Table S-4) is available for download as an Excel file at <http://www.geochemicalperspectivesletters.org/article1827>.

Table S-4 Supplementary data table. **(a)** EMP major element analyses of clinopyroxene. **(b)** EMP major element analyses of plagioclase. **(c)** LA-ICPMS trace element analyses of clinopyroxene. **(d)** LA-ICPMS trace element analyses of plagioclase. **(e)** TIMS neodymium and strontium isotope analyses of plagioclase and clinopyroxene crystals. **(f)** TIMS neodymium isotope analyses of reference material.

Supplementary Information References

- Carlson, R.W., Boyet, M., Horan, M. (2007) Chondrite barium, neodymium, and samarium isotopic heterogeneity and early earth differentiation. *Science* 316, 1175-1178.
- Charlier, B.L.A., Ginibre, C., Morgan, D., Nowell, G.M., Pearson, D.G., Davidson, J.P., Ottley, C.J. (2006) Methods for the microsampling and high-precision analysis of strontium and rubidium isotopes at single crystal scale for petrological and geochronological applications. *Chemical Geology* 232, 114-133.
- Font, L., van der Peijl, G., van Wetten, I., Vroon, P., van der Wagt, B., Davies, G. (2012) Strontium and lead isotope ratios in human hair: investigating a potential tool for determining recent human geographical movements. *Journal of Analytical Atomic Spectrometry* 27, 719-732.
- Griffin, W., Powell, W., Pearson, N., O'Reilly, S. (2008) GLITTER: data reduction software for laser ablation ICP-MS. *Laser Ablation-ICP-MS in the Earth Sciences. Mineralogical Association of Canada Short Course Series* 40, 204-207.
- Griselin, M., Van Belle, J., Pomies, C., Vroon, P., Van Soest, M., Davies, G. (2001) An improved chromatographic separation technique of Nd with application to NdO+ isotope analysis. *Chemical Geology* 172, 347-359.
- Jochum, K.P., Nohl, U., Herwig, K., Lammel, E., Stoll, B., Hofmann, A.W. (2005) GeoReM: a new geochemical database for reference materials and isotopic standards. *Geostandards and Geoanalytical Research* 29, 333-338.
- Kempton, P.D., Hunter, A.G. (1997) A Sr-, Nd-, Pb-, O-isotope study of plutonic rocks from MARK, Leg 153: implications for mantle heterogeneity and magma chamber processes. *Proceedings of the Oceanic Drilling Program Scientific Results* 153, 305-319.
- Klaver, M. (2016) *Dynamics of magma generation and differentiation in the central-eastern Aegean arc*. PhD thesis, Vrije Universiteit, Amsterdam.
- Klaver, M., Smeets, R., Koornneef, J.M., Davies, G., Vroon, P. (2016) Pb isotope analysis of ng size samples by TIMS equipped with a 10^{13} Ω resistor using a ^{207}Pb - ^{204}Pb double spike *Journal of Analytical Atomic Spectrometry* 31, 171-178.
- Koornneef, J., Bouman, C., Schwieters, J., Davies, G. (2014) Measurement of small ion beams by thermal ionisation mass spectrometry using new 10^{13} Ohm resistors. *Analytica Chimica Acta* 819, 49-55.
- MacLeod, C.J., Yaouancq, G. (2000) A fossil melt lens in the Oman ophiolite: Implications for magma chamber processes at fast spreading ridges. *Earth and Planetary Science Letters* 176, 357-373.
- Pollington, A.D., Baxter, E.F. (2011) High precision microsampling and preparation of zoned garnet porphyroblasts for Sm–Nd geochronology. *Chemical Geology* 281, 270-282.
- Sneeringer, M., Hart, S.R., Shimizu, N. (1984) Strontium and samarium diffusion in diopside. *Geochimica et Cosmochimica Acta* 48, 1589-1608.
- Stracke, A., Scherer, E.E., Reynolds, B.C. (2014) Application of Isotope Dilution in Geochemistry. In: Holland, H.H., Turekian, K.K. (Eds.) *Treatise on Geochemistry*. Second Edition, Elsevier, Oxford, 71-86.
- Thirlwall, M. (1991) Long-term reproducibility of multicollector Sr and Nd isotope ratio analysis. *Chemical Geology: Isotope Geoscience section* 94, 85-104.
- Thomas, R. M. (2003) *Processes of lower crustal accretion beneath intermediate- to fast-spreading ocean ridges: constraints from the Wadi Abyad section of the Oman ophiolite*. PhD thesis, Cardiff University.
- Trinquier, A. (2014) Gain calibration protocol for 10^{13} Ω resistor current amplifiers using the certified neodymium standard JNdi-1 on the TRITON Plus. *Thermo Fischer Scientific Technical Note* 30285.
- Wendt, I., Carl, C. (1991) The statistical distribution of the mean squared weighted deviation. *Chemical Geology: Isotope Geoscience section* 86, 275-285.

